



**Anderson, Pamela and Macdonald, Malcolm (2011) Extension of the Molniya orbit using low-thrust propulsion. In: Spaceflight Mechanics 2011. Advances in the Astronautical Sciences, 140, Part . Univelt Inc, pp. 1943-1962. ISBN 978-0-87703-569-5 ,**

This version is available at <https://strathprints.strath.ac.uk/29461/>

**Strathprints** is designed to allow users to access the research output of the University of Strathclyde. Unless otherwise explicitly stated on the manuscript, Copyright © and Moral Rights for the papers on this site are retained by the individual authors and/or other copyright owners. Please check the manuscript for details of any other licences that may have been applied. You may not engage in further distribution of the material for any profitmaking activities or any commercial gain. You may freely distribute both the url (<https://strathprints.strath.ac.uk/>) and the content of this paper for research or private study, educational, or not-for-profit purposes without prior permission or charge.

Any correspondence concerning this service should be sent to the Strathprints administrator: [strathprints@strath.ac.uk](mailto:strathprints@strath.ac.uk)

## EXTENSION OF THE MOLNIYA ORBIT USING LOW-THRUST PROPULSION

Pamela Anderson<sup>\*</sup> and Malcolm Macdonald<sup>†</sup>

Extension of the standard Molniya orbit using low-thrust propulsion is presented. These newly proposed, highly elliptical orbits are enabled by existing low-thrust propulsion technology, enabling new Earth Observation science and offering a new set of tools for mission design. In applying continuous low-thrust propulsion to the conventional Molniya orbit the critical inclination may be altered from the natural value of  $63.4deg$ , to any inclination required to optimally fulfill the mission goals. Analytical expressions, validated using numerical methods, reveal the possibility of enabling a Molniya orbit inclined at  $90deg$  to the equator. Fuel optimal low-thrust control profiles are then generated by the application of pseudo spectral numerical optimization techniques to these so-called Polar-Molniya orbits. These orbits enable continuous, high elevation visibility of the Frigid and Neighboring Temperate regions, using only two spacecraft compared with six spacecraft required for coverage of the same area with a conventional Molniya orbit. This can be achieved using existing ion engines, meaning no development in technology is required to enable these new, novel orbits. Order of magnitude mission lifetimes for a range of mass fractions and specific impulses are also determined, and are found to range from 1.2 years to 9.4 years. Where, beyond 9.4 years the outline mass budget analysis for spacecraft of initial masses of 500kg, 1000kg and 2500kg, illustrated there is no longer a capacity for payload for all initial mass of spacecraft.

### INTRODUCTION

Space-based Earth Observation (EO) measurements for climate change and other monitoring applications are of fundamental importance for validation and assimilation into Earth system models; the Committee on Earth Observation Satellites (CEOS) and the Global Climate Observing System (GCOS) has identified twenty-one Essential Climate Variables (ECVs) that are largely dependent on space-based EO<sup>1</sup>. However, it is of note that the vantage points currently used for EO represent only a small subset of those available.

Consequently, this paper examines the use of low-thrust propulsion applied to the conventional Molniya orbit to produce new, novel orbits to enable new EO mission design in a

---

<sup>\*</sup> [pamela.c.anderson@strath.ac.uk](mailto:pamela.c.anderson@strath.ac.uk), PhD Candidate, Advanced Space Concepts Laboratory, University of Strathclyde, Glasgow, Scotland, E.U.

<sup>†</sup> [malcolm.macdonald.102@strath.ac.uk](mailto:malcolm.macdonald.102@strath.ac.uk), or [space@strath.ac.uk](mailto:space@strath.ac.uk), Associate Director, Advanced Space Concepts Laboratory, University of Strathclyde, Glasgow, Scotland, E.U.

similar manner to the extension of the Sun-synchronous orbit for free selection of orbit inclination and altitude using low-thrust propulsion<sup>2</sup>.

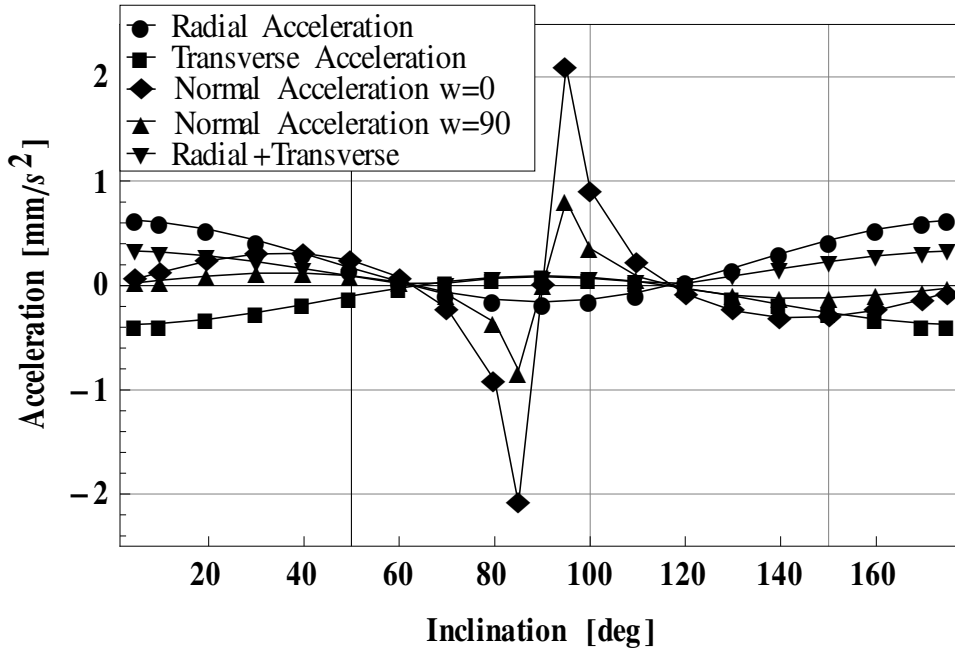
The Molniya orbit is a highly elliptical orbit with a period of 12 hours, at fixed inclination of either *63.4deg* or *116.6deg*. At these unique inclinations the argument of perigee remains fixed, while it will drift due to the oblateness of the Earth at any other inclination.

The paper presents the application of low-thrust propulsion to alter the critical inclination from these conventional values, while maintaining the zero change in argument of perigee condition, essential to the Molniya orbit. Extension of the Molniya orbit using general and special perturbation techniques has previously been introduced<sup>3</sup>, within this paper optimization of these results using pseudo spectral optimization methods is presented, removing the assumptions which were used to generate the initial analytical expressions in Reference 3 to determine, fuel optimal solutions. Following this a mission lifetime analysis is presented, accompanied by a detailed mass budget. In addition to this, a full visibility analysis is presented to show the number of spacecraft required to give continuous observation of a particular region for both the conventional Molniya orbit and a Polar-Molniya orbit.

## **ANALYTICAL RESULTS**

Analytical results have been previously introduced by the authors in Reference 3 to alter the critical inclination of the Molniya orbit to a wide range of values. Expressions combined disturbing forces due to the concentration of mass around the Earth's equator, to the order of  $J_2$  only<sup>4</sup>, and low-thrust perturbations used to artificially alter the magnitude of the  $J_2$  perturbations<sup>3</sup>.

Initially analytical expressions were solved applying continuous low-thrust in each individual direction before accelerations were combined in multiple directions. Considering each acceleration direction in turn, to solve for the acceleration magnitude required to reach inclinations between *5deg* and *175deg*. The possibility of combining an equal and constant magnitude of low-thrust in two of the axial directions was then examined. It was found that combining equal magnitude radial and transverse accelerations reduced the acceleration magnitude from any of the individual directions; this is illustrated in Figure 1.



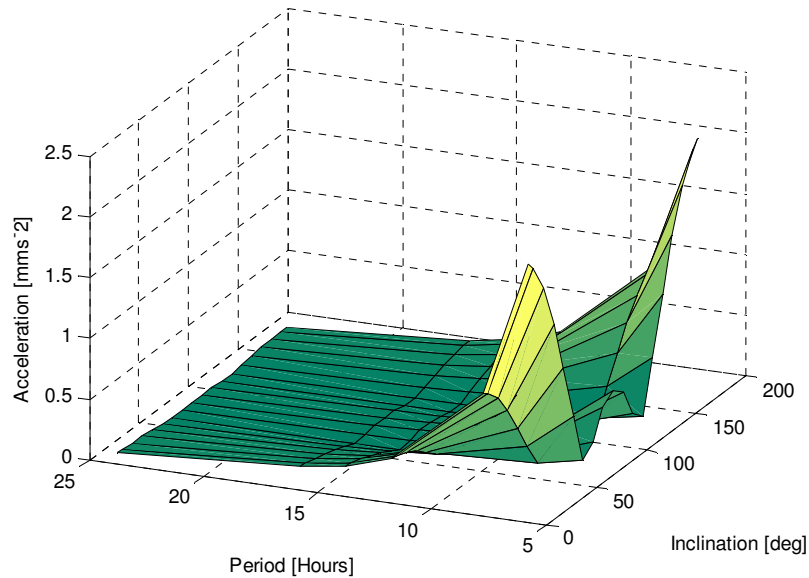
**Figure 1. Thrust Comparison.**

Figure 1 shows the required acceleration using low-thrust propulsion to change the critical inclination of the orbit to a wide range of possible values. It is shown that combining constant continuous radial and transverse thrusts reduced the acceleration magnitude required to achieve any inclination. Figure 1 illustrates that to reach an inclination of  $90deg$  by thrusting in any single direction a transverse acceleration of  $0.0942mm s^{-2}$  is the lowest acceleration required; however, the total acceleration magnitude is reduced to  $0.0834 mm s^{-2}$  by combining equal radial and transverse accelerations.

However, assumptions were made in obtaining these analytical solutions, meaning that the solutions are not optimal, for example assuming the acceleration magnitude was constant and equal in each direction, when in reality the fraction of the total acceleration in each direction would change around the orbit, depending on the true anomaly. Combining the normal acceleration with equal magnitude of radial or transverse acceleration does not necessarily reduce the acceleration magnitude from any of the individual directions, the reason being that the assumption that the magnitude of thrust is the same in each direction forces the solution to thrust in a direction that is not optimal. However, the problem of combining normal acceleration is overcome in the optimized solution, where the assumption of equal acceleration magnitude in each direction is no longer made.

Analytical expressions were also developed for the remaining orbital elements, semi-major axis, eccentricity, inclination and ascending node angle. This process proved that not only was the change in argument of perigee zero over one orbital revolution, but that all other orbital elements were also unaffected by the applied low-thrust.

The technique used to apply low-thrust to alter the inclination of the Molniya-orbit can be used in the same way to modify the critical inclination of highly elliptical orbits with various different orbit periods, for example an orbit with a period of *24 hours*, known as the Tundra-orbit. The results of this process for orbit periods between *6 and 24 hours* are shown in Figure 2.



**Figure 2. Combined Radial and Transverse Thrust.**

Figure 2 shows the results of combining equal radial and transverse accelerations to alter the inclination of a range of orbit periods, with lower orbital periods requiring larger total accelerations than higher period orbits.

## NUMERICAL RESULTS

Analytical results were validated using a numerical simulation, using MatLab software. The numerical model propagated the spacecraft position, by integrating a set of Modified Equinoctial Elements<sup>5</sup>, using an explicit, variable step size Runge Kutta (4,5) formula, the Dormand-Price pair (a single step method)<sup>6</sup>. Numerical simulations included perturbations only due to Earth oblateness, to the order of  $J_2$  only, and results were found to validate the analytical expressions. The numerical model proved that not only was the change in argument of perigee negligible due to the applied low-thrust, but the change in all other orbital elements also matched the analytical results, illustrated in Figure 3.

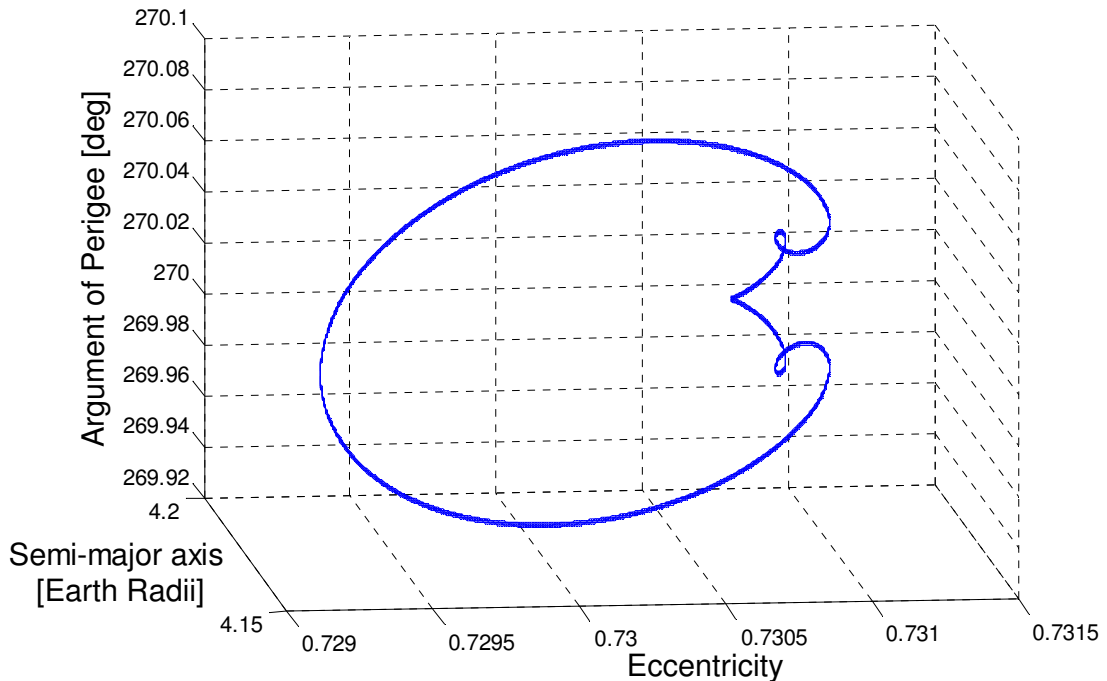


**Figure 3. Variation of Argument of Perigee, Eccentricity and Semi-Major Axis over the Polar-Molniya orbit.**

Figure 3 illustrates the variation in orbital elements over seven orbital revolutions of the Polar-Molniya orbit with a total acceleration of  $0.0834\text{mm/s}^2$  split equally between radial and transverse directions. Examination of the plot shows that although semi-major axis, eccentricity and argument of perigee oscillate during one orbit, all orbital elements return to the same initial value. Examination of the inclination and ascending node angle showed no variation of these parameters over an orbital revolution.

## NUMERICAL OPTIMISATION RESULTS

The problem becomes more complex when low-thrust normal to the orbit plane is included, meaning it is no longer possible to obtain general analytical solutions. A number of assumptions have also been made to attain the general analytical solutions; consequently the results are far from optimal. A Pseudospectral Optimal Control Solver (PSOPT) was then used to determine a numerically optimal solution combining the thrust in all three axial directions. The assumption that the fraction of the total acceleration was the same in each direction was no longer made; hence a fuel optimal solution was determined.

PSOPT uses direct collocation methods, including pseudo spectral and local discretizations to solve optimal control problems by approximating the time-dependent variables using polynomials. The goal of the problem was to compute an optimal low-thrust policy for a spacecraft to maintain a Polar-Molniya orbit, while maximising the final mass of the spacecraft.

The initial guess for the optimization was generated by the general perturbations solution which was then used as the basis for a numerical simulation using special perturbations

techniques; the result of the special perturbations analysis gave the initial guess for the numerical optimization. The optimization uses a set of Modified Equinoctial Elements<sup>5</sup> and a spacecraft with initial mass of  $1000kg$ , specific impulse of  $4600sec$ , and total acceleration of  $0.0834mms^{-2}$ . The analysis was initially conducted including perturbations due to the oblateness of the Earth to the order of  $J_2$  only, this was then extended to include perturbations of the order of  $J_4$  and no meaningful difference was found in the results. The optimal solution was obtained using 17 nodes and the resulting control profiles over time in the radial, transverse and normal directions respectively are shown.

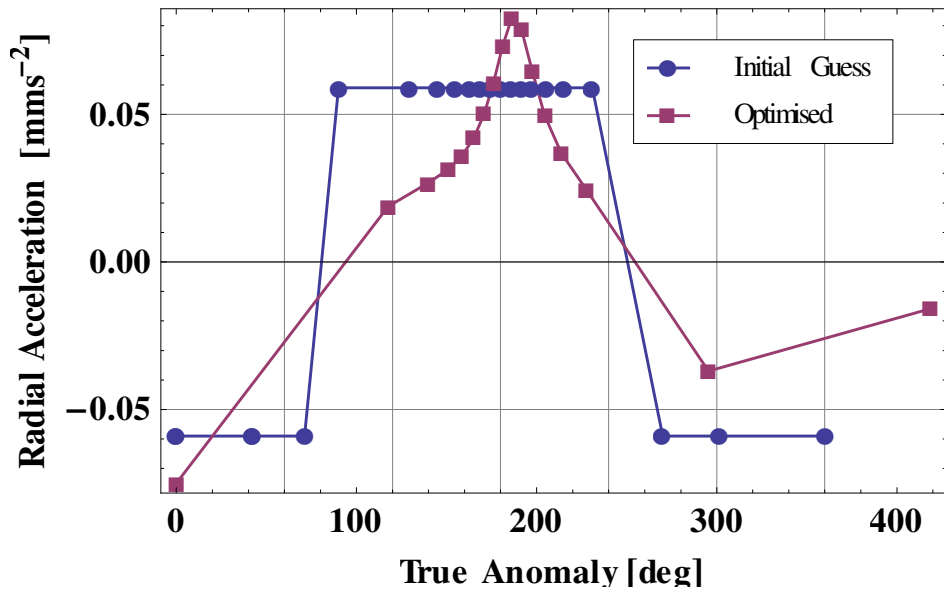


Figure 4. Radial Control Profile.

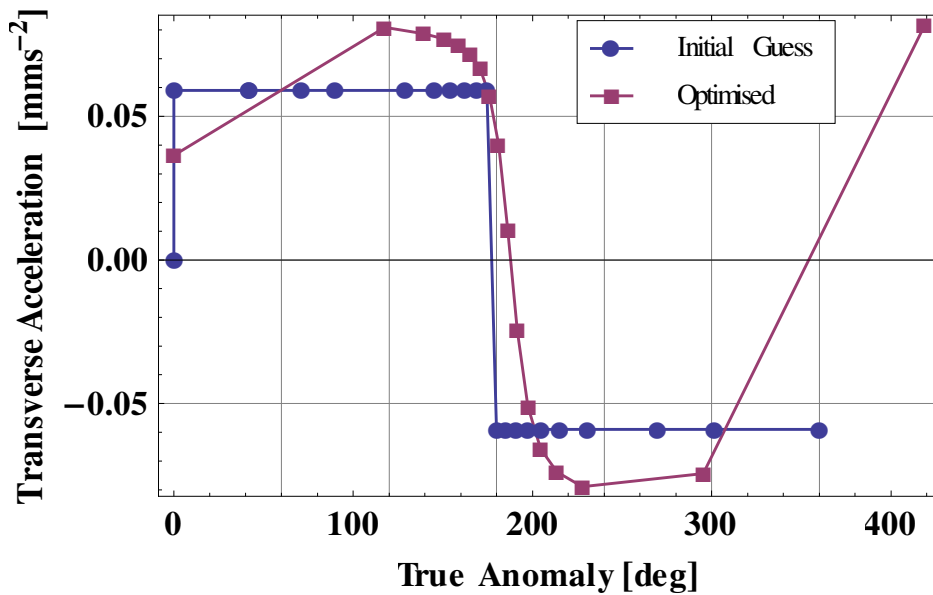
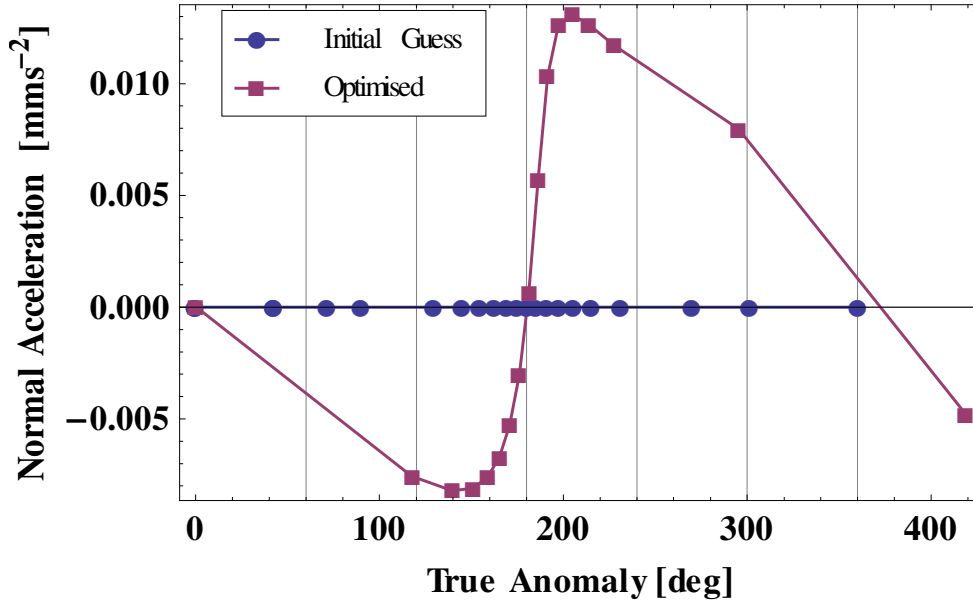


Figure 5. Transverse Control Profile.



**Figure 6. Normal Control Profile.**

The control profiles show that as the assumption of equal acceleration magnitude is no longer made the total acceleration is now composed of radial, transverse and normal components, with the fraction of total acceleration in each direction changing with true anomaly.

To complete one revolution of the Polar-Molniya orbit, the special perturbations solution required a fuel mass of 80.4g, while the optimal solution requires only 77.5g, a 3.6% saving in fuel consumption.

### MISSION LIFETIME

This section looks at finding the possible mission lifetime of a Polar-Molniya spacecraft using a Solar Electric Propulsion (SEP) system; this is done by evaluating the performance in terms of propellant consumption. Starting with the differential equation for the mass of the spacecraft,

$$\dot{m} = -\frac{T}{I_{sp}g_0} \quad (1)$$

Where, T is the thrust magnitude of the SEP system,  $I_{sp}$  is the specific impulse and  $g_0$  is the Earth gravity constant, where the thrust is found using:

$$T = a_p m \quad (2)$$

Where  $a_p$  is the constant acceleration of the SEP system, and m is the mass. Substituting Equation (2) into Equation (1) and rearranging gives the following integral:



$$\int_{m_0}^{m_f} \frac{dm}{m} = - \int_{t_0}^{t_f} \frac{a_p}{I_{sp} g_0} dt \quad (3)$$

Evaluating the integrals, with  $t_f = 0$ , results in:

$$L = t_f = - \ln \left( \frac{m_f}{m_0} \right) \frac{I_{sp} g_0}{a_p} \quad (4)$$

Where the mass fraction  $m_f/m_0$  is defined as,

$$\frac{m_f}{m_0} = \frac{(m_0 - m_{prop})}{m_0} \quad (5)$$

The lifetime of the mission can then be determined for a particular mass fraction, specific impulse and constant acceleration. Using the total acceleration required to achieve the Polar-Molniya orbit, taking into the consideration the percentage fuel saving following optimization, of  $0.0804 mms^{-2}$  and a wide range of mass fractions and specific impulses ranging from currently feasible values to far term technologies, results in the following surface plot:

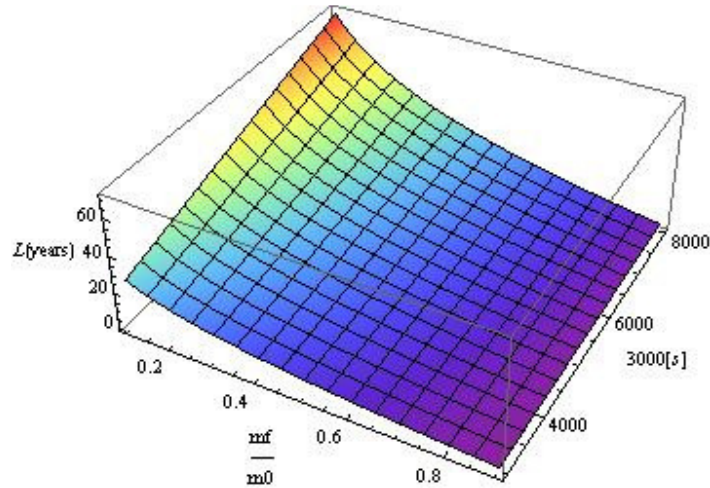


**Figure 7. Mission Lifetime of Polar-Molniya Orbit.**

Figure 7 shows the mission lifetime ranges from around *1.22 years* to around *71.2 years* to maintain the Polar-Molniya orbit; for example using a specific impulse of *3000s* and mass fraction of *0.5* results in a mission lifetime of *8.04 years*.

## MASS BUDGET

A mass budget analysis is conducted to determine the mass of the propellant and power systems required for a Polar-Molniya orbit of a given duration. Hence, for a specified initial mass of spacecraft, the remaining mass of the spacecraft system, including payload, is determined. The initial mass of the spacecraft is composed of many elements<sup>7</sup>:

$$m_0 = m_{prop} + m_{tank} + m_{SEP} + m_p + m_{pay} \quad (6)$$

Where,  $m_0$  is the initial spacecraft mass,  $m_{pay}$  is the remaining mass, including payload, and  $m_{prop}$  is the propellant mass for a given mission duration, found by:

$$m_{prop} = m_0 - m_f \quad (7)$$

Where  $m_f$  is the final mass of the spacecraft, using Equation(2), the final mass can be approximated by:

$$m_f = m_0 - \frac{T_{max}}{I_{sp} g_0} \Delta t \quad (8)$$

Where  $\Delta t$  is the mission duration, combining Equations (7) and (8) results in the following expression for propellant mass over a given time:

$$m_{prop} = \frac{T_{max}}{I_{SP} g_0} \Delta t \quad (9)$$

From Equation (6),  $m_{tank}$  is the mass of the propellant tanks, which is a function of the propellant mass and is found by<sup>[8]</sup>,  $m_{tank} = 0.1m_{prop}$ . The mass of the SEP thruster,  $m_{SEP}$  is a function of the maximum power of the SEP system,  $P_{max}$ . The mass of the SEP thruster is found by:

$$m_{SEP} = k_{SEP} P_{max} \quad (10)$$

Where the maximum power is calculated using:

$$P_{max} = \frac{T_{max} I_{SP} g_0}{2\eta_{SEP}} \quad (11)$$

With the specific performance of the thruster<sup>9</sup>,  $k_{SEP} = 0.02 \text{ kg/W}$  and the thruster efficiency<sup>10</sup>  $\eta_{SEP} = 0.7$ . In Equation (6),  $m_p$  is the mass of the system that provides electrical energy to the SEP system, using a solar array, the mass is:

$$m_p = k_{SA} P_{max} \quad (12)$$

With the specific performance of the solar array<sup>11</sup>,  $k_{SA} = 1/45 \text{ kg/W}$  and  $P_{max}$  found using Equation (11). The unknowns in Equation (6) are then, the payload mass, the initial mass, the specific impulse, the maximum available thrust and mission duration. For an SEP system, the maximum available thrust occurs at time  $t=t_0$ . The initial mass is then found by:

$$m_0 = \frac{T_{max}}{a} \quad (13)$$

Using an acceleration of  $0.0804 \text{ mms}^{-2}$ , the maximum initial mass is found as a function of maximum thrust, the results are shown in Figure 8.

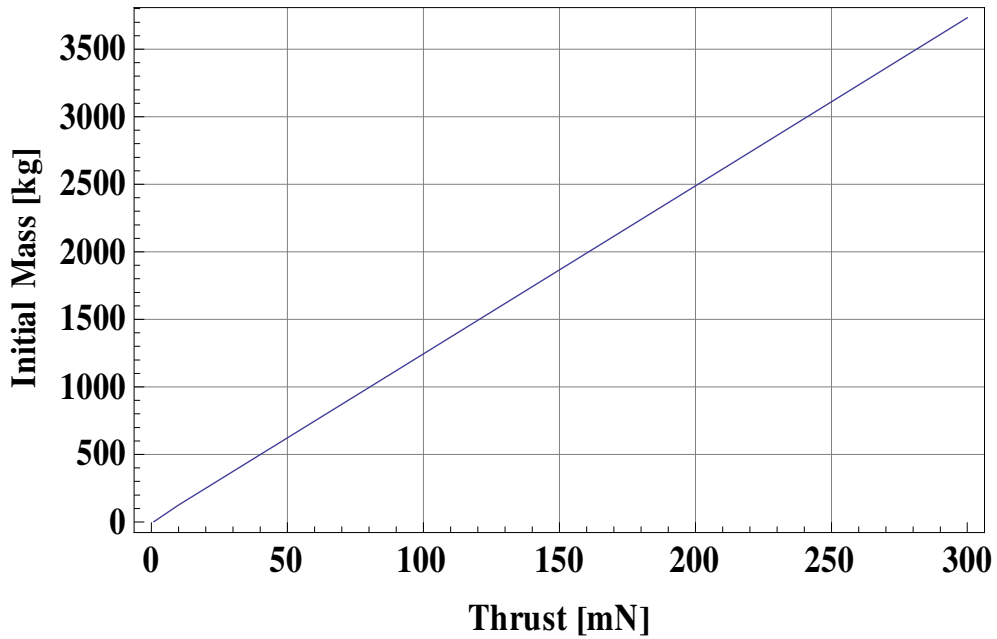


**Figure 8. Maximum Initial Mass as a Function of Maximum thrust.**

Using Figure 8 and selecting various initial spacecraft masses, for example spacecraft with initial mass of *500kg*, *1000kg* and *2500kg*, give maximum thrust values of *40.2mN*, *80.4mN* and *201mN* respectively. Assuming a specific impulse of *3000s*, substituting the appropriate values into Equation (6) and solving for the available remaining mass for each of the spacecraft masses for a range of mission lifetimes results in the following available payload masses.

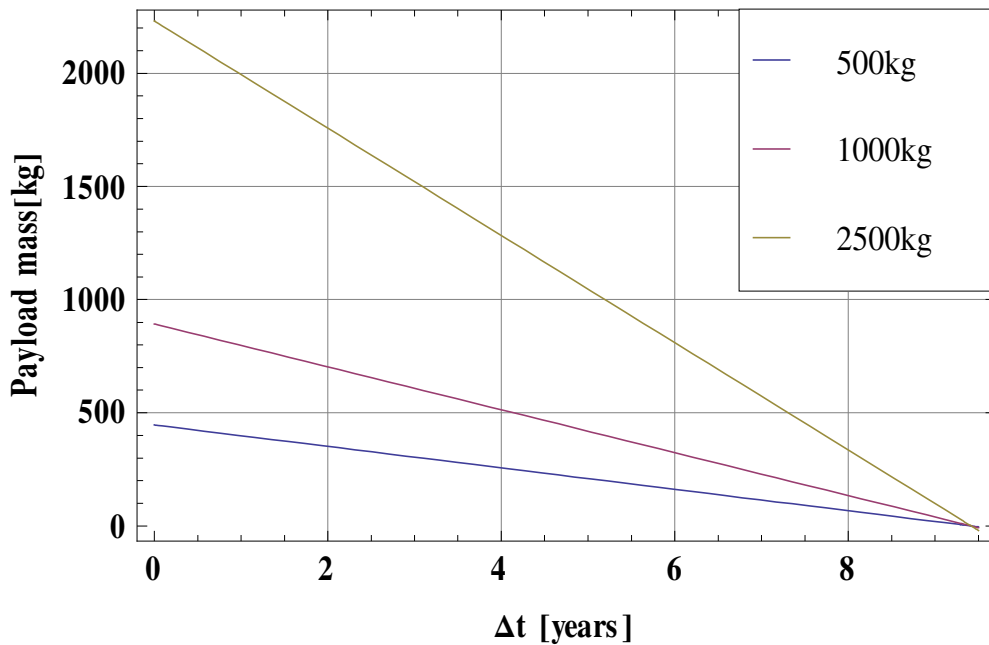


**Figure 9. Payload Mass as a Function of Mission Lifetime.**

Figure 9 shows the available remaining mass, including payload for each initial mass of spacecraft as a function of mission lifetime. Note that for mission durations above 9.5 years there is no allowance for payload mass, as the propellant mass becomes too large.

Although the orbit requires a constant acceleration, as the propellant is consumed and the propellant mass decreases, the acceleration will increase from the SEP system. A variable thrust SEP system is therefore required; the thrust range necessary from the SEP system can be determined by finding the thrust at the beginning of the mission, with all the propellant, and the thrust at the end of the mission, with zero propellant. These thrust ranges are shown for the three initial mass of spacecraft previously considered, for a range of mission lifetimes.

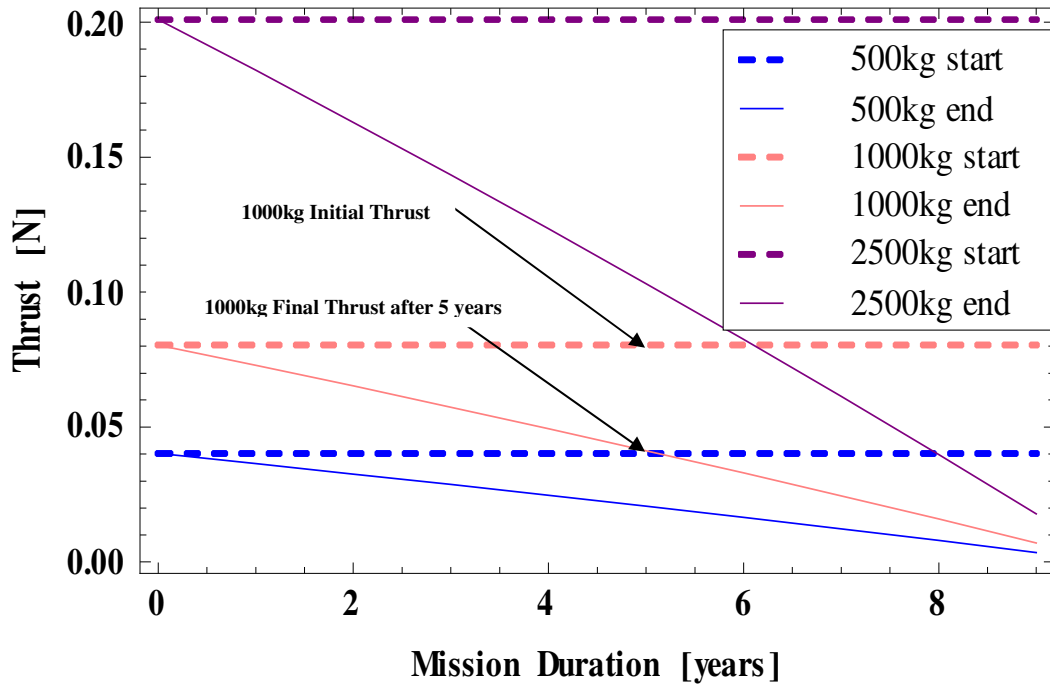


**Figure 10. Thrust Ranges for Variable SEP System.**

Considering the 1000kg spacecraft with mission duration of 5 years the thrust at the beginning of the mission, with all propellant is 80.4mN and at the end of this mission, with zero propellant, is 41.3mN. The thrust range required by the system could be provided by various technologies, such as ion engines, one example which could achieve the desired thrust range is the QinetiQ T6 thruster, which is throttleable between 30mN and 210mN<sup>12</sup>. Another example of a thruster which can provide adequate thrust is NASA’s Solar Electric Propulsion Technology Application Readiness (NSTAR) thruster, which has undergone significant ground testing in addition to a flight test on the Deep Space 1 (DS1) spacecraft<sup>13</sup>, and is capable of providing between 20mN and 94mN of thrust.

### VISIBILITY ANALYSIS

A full visibility analysis is conducted to determine the number of spacecraft required on the Polar-Molniya orbit to give complete coverage of the Frigid and neighboring Temperate zones.

The same process is also carried out for the conventional Molniya orbit in order to draw comparison between the number of spacecraft required for continuous observation of this region.

This is achieved by determining the time a spacecraft on either the traditional Molniya orbit or the Polar-Molniya orbit can view ground stations positioned at  $10deg$  longitude intervals at particular latitude. This is accomplished by calculating the maximum elevation angle for each ground station while assuming a value for the corresponding minimum elevation angle, between this ranges, the spacecraft is in view of the ground station, where the parameters are introduced in Figure 11. The coverage for a number of spacecraft over time is then plotted to determine the number of spacecraft required for continuous observation of a given region. The region considered was above  $55deg$  latitude, and employed a minimum elevation angle of  $20deg$ . The results of this process for the conventional Molniya and Polar-Molniya orbit are shown in Figure 12 and Figure 13 respectively.

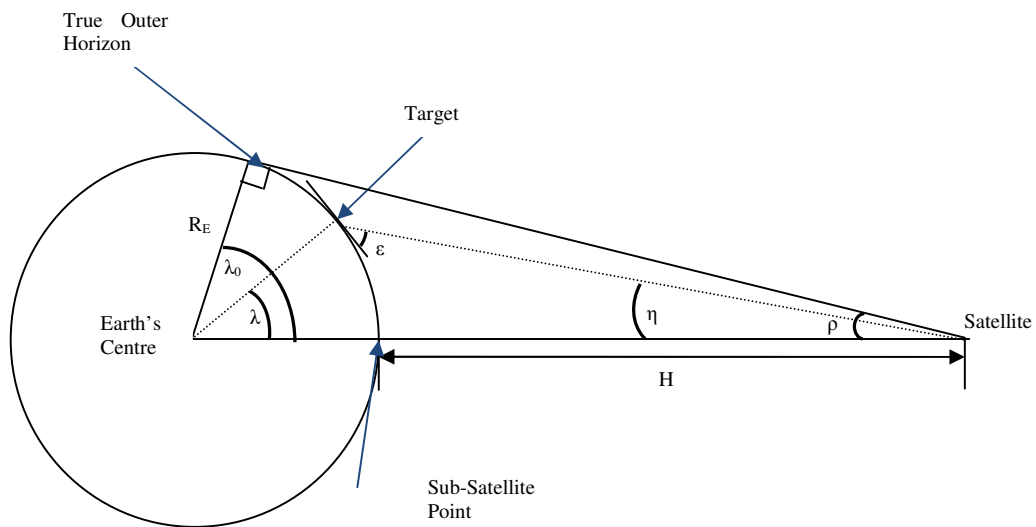


**Figure 11. Angular Relationships between Satellite, Target and Earth Centre.**

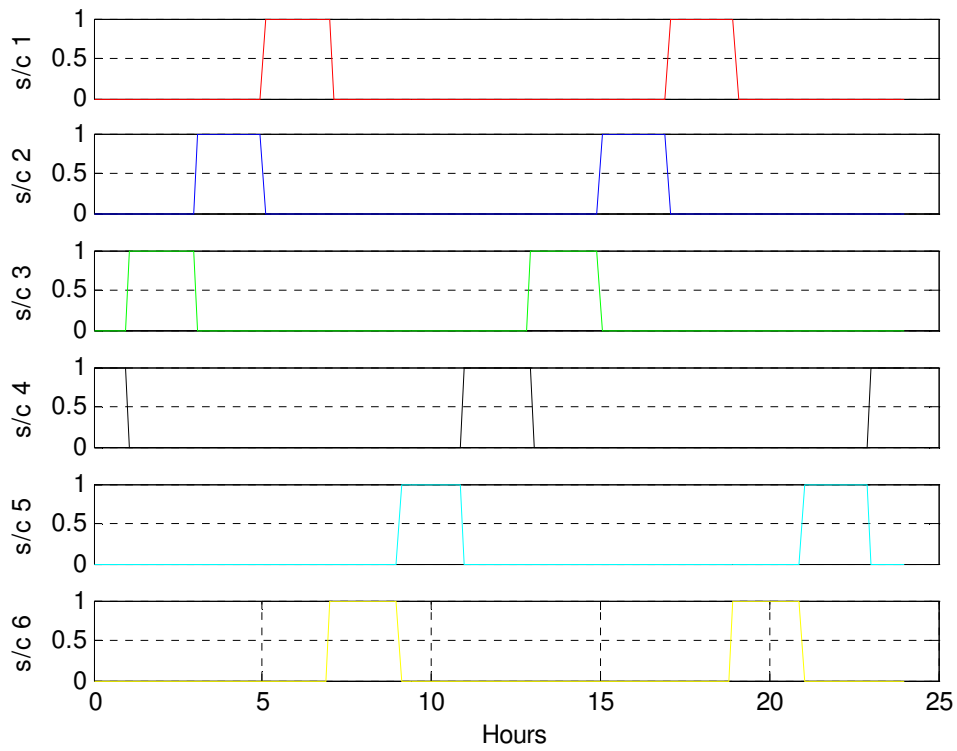


**Figure 12. Molniya Observation above 55deg.**

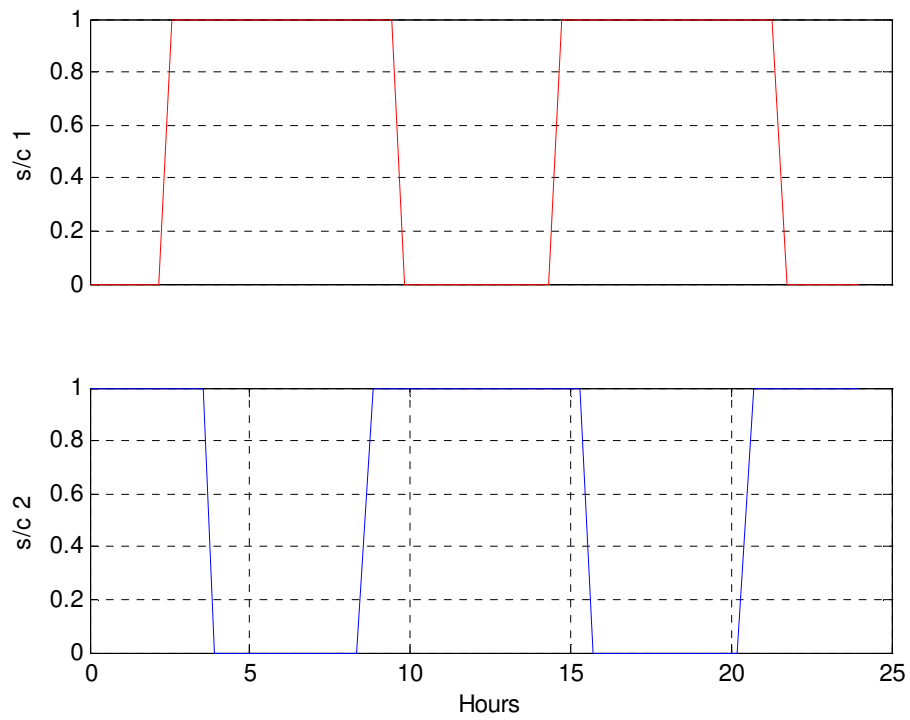


**Figure 13. Polar-Molniya Observation above 55deg.**

Figure 12 shows that to provide continuous coverage of regions above  $55deg$ , with a minimum elevation angle of  $20deg$ , requires six spacecraft, equally spaced around the traditional Molniya orbit, this is compared to only two spacecraft, equally spaced, on the Polar-Molniya orbit to provide the same coverage of this region. The configuration of spacecraft required on the Molniya orbit is shown in Figure 14.

1<sup>st</sup> - red, 2<sup>nd</sup> - blue, 3<sup>rd</sup> - green, 4<sup>th</sup> - black, 5<sup>th</sup> - cyan, 6<sup>th</sup> - yellow

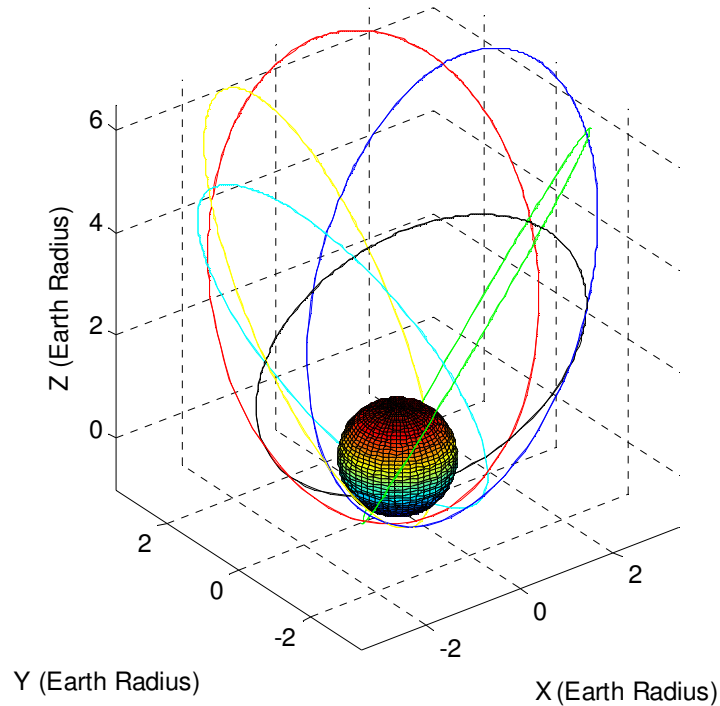


**Figure 14. Conventional Molniya Orbit, Six Spacecraft.**

Although Figure 14 shows six spacecraft with equally spaced ascending node values, it is important to note that this parameter does not have an effect on the coverage provided by the spacecraft. Each spacecraft could in fact have the same value of ascending node, and thus be launched on a single launch vehicle, significantly reducing the overall cost. The same is true for spacecraft on the Polar-Molniya orbit.

A relatively high minimum elevation angle has been stated in this analysis; the basis for this is the increasingly oblique Observational Zenith Angle (OZA) as latitude increases, when viewed from Geostationary orbit (GEO) altitude. Thus, using a minimum elevation of  $20deg$  for the Molniya orbits ensures that these orbits, at the very least, provide data of equal quality of that produced by Geostationary systems.

Visibility analysis including these lower latitude regions is beneficial for several reasons, one of which is the limitation of Geostationary platforms at latitudes above  $55deg$ , which includes, for example, the northern one-third of the UK<sup>14</sup>, this is due to the rapidly decreasing horizontal resolution and increasingly oblique viewing angle. Limitations even begin to appear in Geostationary coverage at latitudes above  $45deg$ . depending on the relative satellite position and

hemispherical location<sup>14</sup>. As such, the breadth and depth of climate and meteorological data which is available for the tropics and mid-latitudes must be approximated by composite or mosaic images beyond around  $55deg$ <sup>15</sup>. Even with the large number of spacecraft required to provide a data refresh rate of 15 minutes, as is typically required for so-called continuous metrological observations, the data would be discontinuous in time and viewing geometry. Such composites are therefore, at best, a compromise, leaving critical climate and meteorological datasets lacking the desired coverage of key polar and temperate regions that is required for validation of Earth system models and near real-time monitoring.

## VISUALISATION OF ORBIT

As explained previously in the visibility analysis, a spacecraft on the Polar-Molniya orbit spends a large amount of time above the Frigid Zone, as a result of apogee dwell, this is demonstrated in Figure 15, which also includes, for comparison a standard Molniya-orbit.

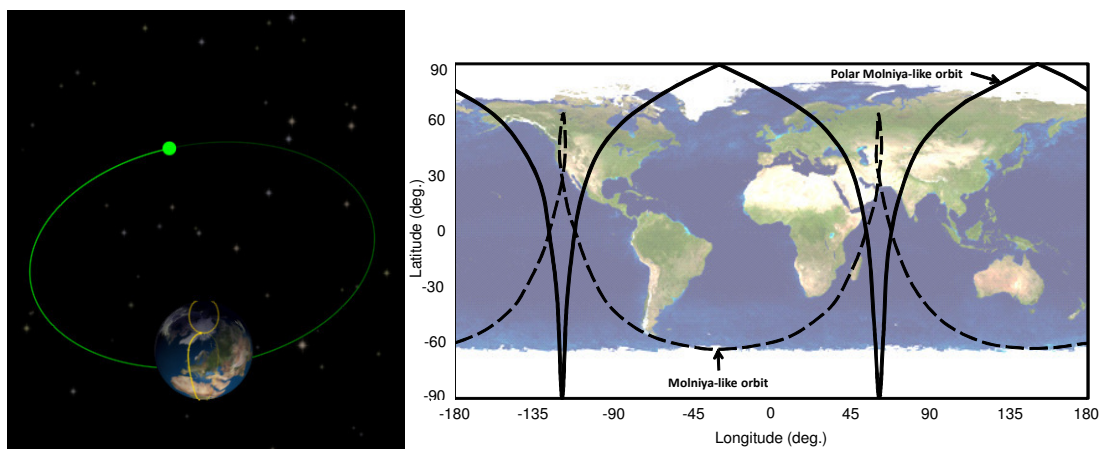


**Figure 15. Visualisation of Polar-Molniya Orbit.**

Spacecraft on a highly elliptical orbit with an inclination of  $90deg$  are beneficial for many reasons, in particular for Earth Observation missions for example, to monitor the rapidly changing environment of the Northern Frigid zone, where at the North Pole the effects of climate change are both amplified and accelerated. Since the end of ICESat in April 2010, there is a greater need for observation of Frigid and neighbouring temperate zones. There is also increasing demand for reliable communication and data relay in the remote polar-regions, The European Space Agency have reinforced this requirement, with the possibility of the Arctic Ocean being utilised as an International shipping route, demanding reliable means of communication, with other services such as tourism, Government services, maritime, aeronautical, offshore and oil and gas also insisting on satellite communication\*. Since communication is typically conducted using spacecraft in Geostationary orbits, which becomes impractical at latitudes above  $55deg$ <sup>14</sup>, it is imperative that means of ensuring reliable communications in the Northern Frigid zone are obtained.

\* Esa Technology and Integrated Applications News Page 18<sup>th</sup> November 2010.



Traditionally, Polar observation is conducted using a Sun-synchronous orbit, where Earth imaging is conducted taking measurements over a strip building up an image of a particular location. The problem associated with these orbits is that the temporal resolution provided is insufficient, this is improved using satellites on a Geostationary orbit; however these Geostationary systems are unable to view deep Polar Regions. Hence, Polar imaging has in the past been achieved by creating a mosaic of both satellite images<sup>16</sup>. This process gives a general summary of weather patterns for a period, but does not give a completely accurate representation, as the image is not continuous.

The American Icesat satellite, used to measure ice sheet mass balance, cloud and aerosol heights in addition to land topography, was inclined at  $94deg$  to the equator. The field of view of the instruments meant that coverage of this spacecraft was only to  $86deg$  north, which left large gaps in Arctic information. These gaps are reduced by Cryosat-2, which is inclined at  $92deg$  and is used to map the ocean circulation of the Arctic basin. Coverage increases using Cryosat-2 which can view to  $88deg$  North. Although both spacecraft have been used to observe Arctic and neighboring temperate regions neither of these spacecraft are true Polar orbits, as a result complete coverage of the Polar caps is compromised, thus highlighting the benefit of true Polar orbits such as the Polar-Molniya orbit.

The Molniya orbit overcomes some of the problems associated with imaging of high latitude regions, as shown in Figure 16.

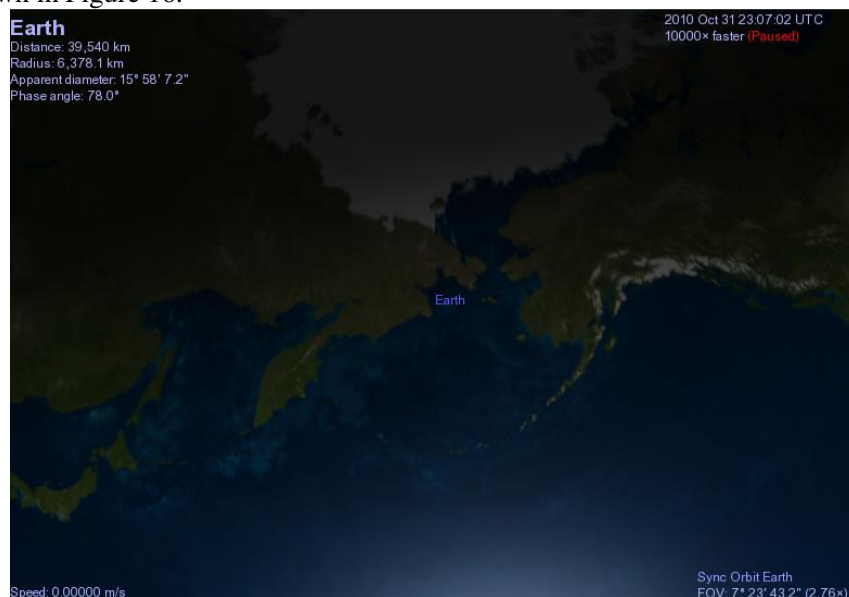


**Figure 16. Molniya-orbit.**

Figure 16 shows the view from a spacecraft on the conventional Molniya orbit with an inclination of  $63.4deg$ , using the field of view of the Landsat-7 Enhanced Thematic Mapper Plus. It shows that partial images of the Northern Frigid Zone are possible; however, the entire region is not in view. This is overcome using a spacecraft on a Polar-Molniya orbit, shown in Figure 17.

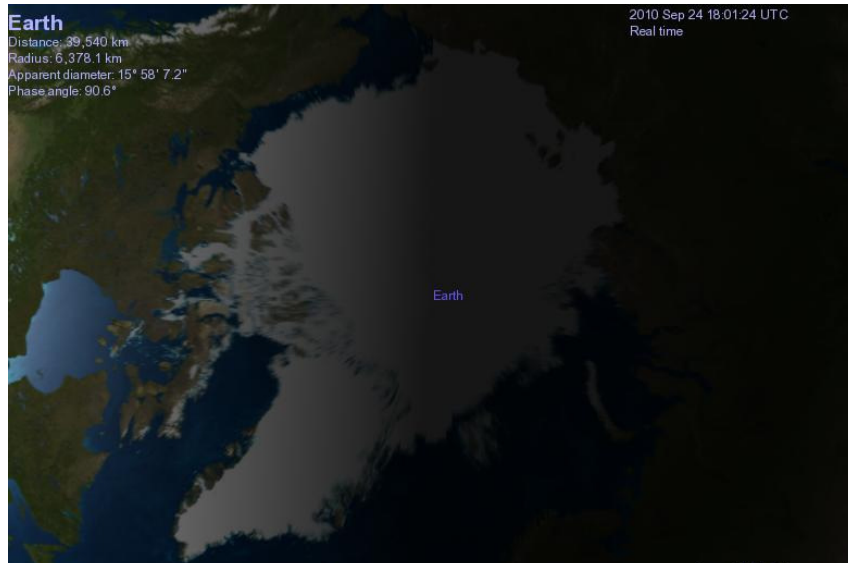


**Figure 17. Polar-Molniya Orbit.**

Figure 17 shows the view from a spacecraft on the Polar-Molniya orbit using the same field of view as the Molniya orbit in Figure 16. It shows that the entire Northern Frigid Zone is now in view, as apogee is now directly above the one of the Earth's poles, the spacecraft can view the Polar Regions for longer periods of time, as demonstrated in the visibility analysis.

An alternative for polar observation is an artificial Lagrange point above one of the Earth's poles<sup>17</sup>, also enabled by continuous low-thrust propulsion. This configuration gives complete hemispherical views throughout the year from a single spacecraft, however to achieve this, the spacecraft must be positioned around 2 – 3 million km above the Earth's surface, giving an equivalent observation capability as illustrated in Figure 18.



**Figure 18. Pole-Sitter.**

Figure 18 shows the view from an artificial equilibrium point in the 3-body problem an altitude of  $2,160,000\text{km}$ , demonstrating the extremely low-resolution from a spacecraft at this altitude with a conventional Earth-observation instrument.

The Polar-Molniya orbit therefore offers continuous observation of the North Pole with fewer spacecraft than Sun-synchronous and traditional Molniya orbits, and at a higher resolution than an artificial equilibrium point in the 3-body problem stationed above the pole, but with two rather than one spacecraft.

## CONCLUSION

The feasibility of using low-thrust propulsion to alter the critical inclination of the Molniya orbit has been illustrated. It was shown that this could be achieved while maintaining the zero change in argument of perigee condition fundamental to this orbit, and ensuring other orbital elements were not adversely affected by the applied low-thrust.

Optimization was carried out to eliminate the assumptions made in obtaining analytical solutions for the extension of the Molniya orbit. This produced control profiles in radial, transverse and normal directions over one orbital revolution to maximize the final mass of the spacecraft. This allowed a higher final mass to be achieved over one orbit from numerical simulations.

Mission lifetime analysis was also performed; this resulted in a range of mission lifetimes for various specific impulses and mass fractions, for example, using a specific impulse of  $3000\text{s}$  and a mass fraction of  $0.5$  results in a mission lifetime of 8.04 years. An outline mass budget was also conducted to determine the mass of the Solar Electric Propulsion system, and power system required for a Polar-Molniya orbit, as such the remaining mass, including payload, for initial spacecraft masses of  $500\text{kg}$ ,  $1000\text{kg}$  and  $2500\text{kg}$  over a range of mission lifetimes up to 9.4 years was established.

Finally, a full visibility analysis was conducted to compare the number of spacecraft necessary to give continuous observation of the Frigid and neighboring Temperate zones from a Molniya orbit and Polar-Molniya orbit. It was found that the Polar-Molniya orbit offers a significant reduction in the number of spacecraft required for observation of Frigid and neighboring Temperate zones. Requiring only two spacecraft to observe to  $55\text{deg}$  latitude, compared to six spacecraft required to view the same region using the conventional Molniya orbit.

In varying the critical inclination of the Molniya orbit, the potential applications are extended. As such continuous, real-time imaging of Polar Regions is enabled using existing or near-term technology. The potential applications of such an orbit include, opportunities for reliable communications in high latitude regions, real-time observation of Frigid and neighboring Temperate zones using fewer spacecraft than traditional Sun-synchronous and Molniya orbits, and more accurate imaging of this region; in turn allowing improvements in climate and weather data.

## ACKNOWLEDGMENTS

This work was part funded by NERC grant reference number NE/1000801/1;SpeCL: Early Concepts for a New Mission: A Spaceborne Multispectral Canopy Lidar.

## NOTATION

|               |   |
|---------------|---|
| $a$           | semi-major axis                                 |
| $a_n$         | normal acceleration                             |
| $a_p$         | solar electric propulsion constant acceleration |
| $a_r$         | radial acceleration                             |
| $a_t$         | transverse acceleration                         |
| $g_0$         | Earth gravity constant                          |
| $H$           | altitude  |
| $I_{SP}$      | specific impulse                                |
| $J_2$         | perturbation due to Earth oblateness            |
| $k$           | specific performance                            |
| $L$           | mission lifetime                                |
| $m$           | mass  |
| $\dot{m}$     | mass flow rate                                  |
| $n$           | mean motion                                     |
| $P$           | power   |
| $R_E$         | mean radius of Earth                            |
| $t$           | time  |
| $T$           | thrust  |
| $\varepsilon$ | elevation angle                                 |
| $\eta$        | nadir angle                                     |
| $\eta_{SEP}$  | thruster efficiency                             |
| $\lambda$     | Earth central angle                             |
| $\mu$         | gravitational parameter of Earth                |
| $\rho$        | angular radius of Earth                         |
| $\omega$      | orbital angular velocity                        |

*SI Units used throughout unless otherwise stated.*

## REFERENCES

- <sup>1</sup> "Global Monitoring of Essential Climate Variables," in *ESA/PB-EO(2009)32*, ed: Esa-Earth Observation Programme Board.
- <sup>2</sup> M. Macdonald, *et al.*, "Extension of the Sun-Synchronous Orbit," *Journal Guidance Control and Dynamics*, vol. In Press, 2010.
- <sup>3</sup> P. Anderson and M. Macdonald, "Extension of Earth Orbits Using Low-Thrust Propulsion," in *61st International Astronautical Congress*, Prague, Czech Republic, 2010.
- <sup>4</sup> D. A. Vallado, *Fundamentals of Astrodynamics and Applications*, Third ed., 2001.

- 5 M. J. H. Walker, *et al.*, "A set of Modified Equinoctial Orbital Elements," *Celestial Mechanics*  
vol. 36, pp. 409-419, 1985.
- 6 J. R. Dormand and P. J. Prince, "A family of embedded Runge-Kutta formulae," *Journal of*  
*Computational and Applied Mathematics and Statistics*, vol. 6, pp. 19-26, 1980 1980.
- 7 M. Ceriotti and C. R. McInnes, "A near term pole-sitter using hybrid solar sail propulsion,"  
presented at the 2nd International Symposium on Solar Sailing, ISSS 2010, New York, USA,  
2010.
- 8 R. Gershman and C. Seybold, "Propulsion Trades for Space Science Missions," *Acta Astronautica*,  
vol. 45, pp. 541-548, 1999.
- 9 J. R. Brophy, "Advanced Ion Propulsion Systems for Affordable Deep-Space Missions," *Acta*  
*Astronautica*, vol. 52, pp. 309-316, 2003.
- 10 S. Kitamura, *et al.*, "Overview and research status of the JAXA 150-mN ion engine," *Acta*  
*Astronautica*, vol. 61, pp. 360-366, 2007.
- 11 J. R. Wertz and W. J. Larson, *Space Mission Analysis and Design* vol. Third Edition: Microcosm  
Press and Kluwer Academic Publishers, 1999.
- 12 N. C. Wallace, "Testing of the Qinetiq T6 Thruster in Support of the ESA BepiColombo Mercury  
Mission," *Proceedings of the 4th International Spacecraft Propulsion Conference (ESA SP-555)*,  
2-9 June 2004.
- 13 J. R. Brophy, *et al.*, "Ion Propulsion System (NSTAR) DS1 Technology Validation Report."
- 14 L. P. Riishojgaard, "Report on Molniya Orbits," presented at the World Meteorological  
Organization Commission for Basic Systems, OPAG on Integrated Observing Systems Expert  
Team on Observational Data Requirements and Redesign of the Global Observing System,  
CBS/OPAGIOS/ODRRGOS-7/Doc.7.5, Seventh Session, Geneva Switzerland, 2004.
- 15 M. A. Lazzara, *et al.*, "Antarctic Satellite Meteorology; Applications for Weather Forecasting,"  
*Monthly Weather Review*, vol. 131, pp. 371-383, 2003.
- 16 M. A. Lazzara, *et al.*, "10 Years of Antarctic Composite Images."
- 17 M. Ceriotti and C. R. McInnes, "A Near Term Pole-Sitter using Hybrid Solar Sail Propulsion,"  
presented at the 2nd International Symposium on Solar Sailing, New York, USA, 2010.